Proceedings of the 17th World Congress
The International Federation of Automatic Control
Seoul, Korea, July 6-11, 2008

Optimal Model Matching Design for High Bandwidth, High Resolution Positioning in AFM ⋆

C. Lee * **S. Salapaka** **

* *Department of Mechanical Sciences and Engineering, University of Illinois, Urbana-Champaign, IL 61801 USA (Tel: 217-265-9449; e-mail: clee62@uiuc.edu).*
** *Department of Mechanical Sciences and Engineering, University of Illinois, Urbana-Champaign, IL 61801 USA (e-mail: salapaka@uiuc.edu)*

Abstract: This paper introduces a two degree of freedom control design for achieving robust high resolution, high bandwidth positioning systems. Feedback designs have demonstrated a significant improvement in the performance of the flexure-stage based positioning systems in atomic force microscopes (AFM) that provide large travels with high resolution. In this paper, an optimal model matching framework, where both the feedback and feedforward controllers form the decision variables, is presented which facilitates achieving better performance in terms of the resolution bandwidth and robustness to modeling uncertainties in the closed-loop device. Feedback-only designs, which significantly diminish nonlinear effects of piezoactuation and other modeling uncertainties, are restricted by practical and fundamental limitations such as the control saturation and the Bode integral law. These limitations, which become even more prominent due to non-minimum phase zeros in the context of flexure stages with non-collocated actuators and sensors, typically lead to trade-off between resolution, bandwidth and the robustness of the positioning system. A two degree of freedom controller, achieves a better trade-off by exploiting feedforward designs that are not subject to some limitations that constrain the feedback-only designs. We show that our 2DOF design achieves performance objectives that are impossible for feedback-only designs. Experiments on positioning stages on a AFM show bandwidth improvements as large as 300% over existing feedback base designs.

1. INTRODUCTION

Scanning probe microscopes (SPM) such as scanning tunneling microscope (STM) and atomic force microscope (AFM) form one of the main reasons for the recent rapid growth in nanoscience and nanotechnology. Among SPMs, AFM is most widely used due to its versatility in terms of its operability in wide temperature or pressure range, invulnerability to magnetic fields, and its capability to probe a wide variety of materials. In a typical AFM, a sample image is obtained by a probe (microcantilever tip) that traces the topography of a sample as the sample is moved laterally under it by a positioning system (scanner). AFM has enabled research in diverse areas such as biology, materials science, optics, precision mechanics, and microelectronics (Bhushan (1999)) and this research, in turn, has imposed new demands on resolution, bandwidth and reliability. Applications in material science, biology, semiconductor, and photonics industry require high precision as well as high bandwidth to enable certain science, as in T cell-dynamics studies (Fillmore et al. (2003)), to keep up with the high throughput requirements. These applications demand robustness in high resolution fast scanning in terms of reliability in the context of various operating environments, conditions and modeling uncertainties.

⋆ This work was supported by National Science Foundation Grant No. ECS 0449310 CAR.

Precision in positioning plays an important role in performance of AFM since typically positioning systems have relatively lower open-loop bandwidth (typically an order or more smaller) than cantilevers and thus accuracy in positioning decides the quality of images in AFM. Generally, AFM scanner uses piezoelectric actuators since they provide high precision (sub-nanometer scale), have fast response, have no backlash and no wear, require little maintenance, provide relatively large forces, are invulnerable to magnetic fields, low temperature and low pressure. However, they suffer from some nonlinear effects such as hysteresis, and creep(Croft et al. (2000)). Many efforts that include feedforward designs and feedback designs have been reported to diminish these nonlinear effects and to improve the performance(Leang and Devasia (2002); Y. and Zou (2007); Daniele et al. (1999); Schitter et al. (2001); Salapaka et al. (2002); Sebastian and Salapaka (2005)). Feedforward designs are very sensitive to accuracy in models and therefore are not very robust to modeling uncertainties, and the current research in this direction focuses on obtaining robust mechanisms. Feedback designs do provide robustness to modeling uncertainties, in addition to improved performance, but are still limited by fundamental limitations that bind them.

In this paper, the design and implementation of feedback together with feedforward controller is presented. This work shares the philosophy of combining the feedforward

and feedback designs as in (Schitter et al. (2004); Y. and Zou (2007)) that reported a two degree of freedom control using the information of the previous scan line as a feedforward signal. However, new design in this research determines a tradeoff between the robustness to modeling uncertainties and bandwidth for a given precision by appropriately formulating and solving an optimal control problem where both the feedback and feedforward laws form the decision variables. This paper provides an improvement over the methodology in (Sebastian and Salapaka (2005)) where robustness of existing feedback designs is guaranteed without any improvement in the positioning bandwidth. The point of the control design in this paper is to show that the robustification of the closed loop system and to increase the bandwidth can be achieved simultaneously. In the following sections, we briefly describe the device and the objective of control and characterize limitations on the feedback design. We show that feedback and forward design individually cannot achieve certain performance specifications on precision, bandwidth and robustness. We present a two degree of freedom robust control design which is motivated by Glover-MacFarlane robustification and model-matching scheme. This design is followed by the analysis and discussion on the results achieved by it.

2. DEVICE DESCRIPTION

The nano-positioning system studied in this article is the 2 dimensional flexure scanner of MFP-3D developed in Asylum Research, Santa Barbara, CA. The flexure scanner consists of two stages (fast axis 'X' stage is located on slow axis 'Y' stage), the serpentine spring which connects the stages and frame without the mechanical contact, stack-piezos for actuation and the linear variable differential transformer (LVDT) sensors (Figure 1(a)). The piezoactuators give a travel range of 90μm in close loop in both directions. The LVDT sensors used have noise less than 0.6nm (standard deviation) over a bandwidth from 0.1 to 1 kHz.

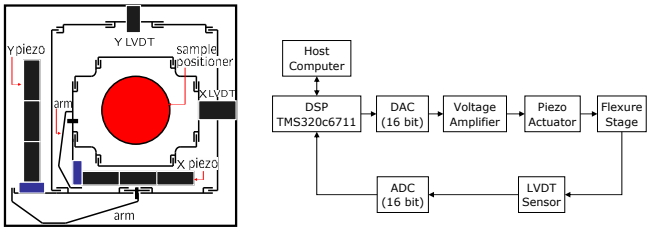

(a) (b)

Fig. 1. (a) Schematic of flexure scanner: The sample is placed on the central block of the flexure stage which is driven by the x-piezo which in turn is driven by the y piezo. The x and y-LVDTs measure the current stage position. (b) Control system setup for flexure stage.

The control law is discretized and implemented on a Texas instrument TMS320C6713 digital signal processor (DSP) using code composer studio with 16bits A/D and 16bits D/A channels. The setup of control system is shown in Figure 1(b).

3. IDENTIFICATION, OBJECTIVES AND LIMITATIONS

3.1 Identification

Physical modeling of the device is difficult due to its complicated structural design and poorly understood piezoactuation phenomena and any attempt in that direction results in complex dynamics and with significant uncertainty in model. Therefore identification techniques were used to derive linear models about an operating point. The frequency-response based identification was performed on the voltage amplifier, the piezoelectric actuator, the flexure stage and the LVDT based sensing mechanism. The sine-sweep identification was done using HP 35670A dynamic signal analyzer with 10mV constant amplitude for frequency range of 1Hz to 2kHz. The small amplitude of voltage (10mV over -10 to 10V input range) is applied to the input of each of the axis so that the local relation between the input and output remains linear. From the identification results, X and Y crosstalk are seen to be relatively small ($\max|G_{xy}| = -17.76$dB) since, by design, X and Y stages are decoupled and are orthogonal to each other. Therefore, the nanopositioning system is modeled by two independent single input single output (SISO) units. The mode of operation of this device is such that higher bandwidth requirements are made on the smaller stage X whereas the Y stage is made to move relatively slow. Hence, there is a greater emphasis on the control designs for the X stage, which is presented in this paper.

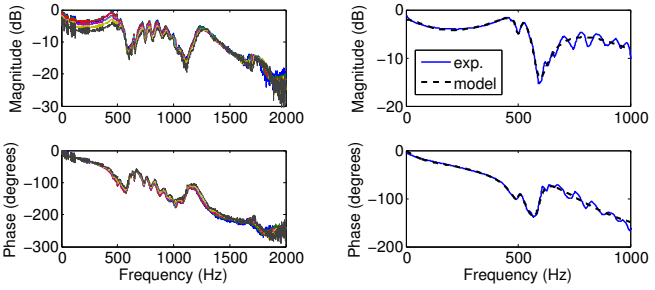

(a) (b)

Fig. 2. (a)Experimental frequency responses at various operating position. (b)Nominal frequency response(solid) and model frequency response(dashed). Low order model response do not capture high freqeuncy dynamics.

Figure 2(a) shows the experimental frequency response results for various operating point. It is observed that the frequency response at the same operating point varies when obtained at different times. These uncertainties motivate the objective requirement of control design. The nominal frequency response of the system is obtained about the nominal operating point which is of DC offset corresponds 0V at output. Figure 2(b) shows a comparison of the fitted mathematical model and nominal experimental result. Iterative least square fitting was performed over $0-1$kHz and the resulting 7th order model is given in the following;

$$G_{xx}(s) = \frac{-730.4691(s-1.363\times10^4)(s+963.6)}{(s+612.9)(s^2+260.5s+9.955\times10^6)} \times \frac{(s^2+156.2s+9.911\times10^6)(s^2+299.8s+1.396\times10^7)}{(s^2+701.4s+1.133\times10^7)(s^2+3253s+2.426\times10^7)} \quad (1)$$

Note that this 7th order model did not capture dynamics over 500Hz. Its use is justified by the fact that the frequency range of interest is less than 500Hz and larger models result in implementations of higher order control which cannot be accommodated by the processor within short sampling time. This modeling uncertainty from using low order model was accounted for by imposing the requirement of making the closed loop system robust to it on the control design.

3.2 Objectives

The objectives of control design in this research are to achieve high bandwidth, high resolution and robustness to modeling uncertainties. The closed loop bandwidth in the untampered commercial system is about 50Hz while the open loop identification (Figure 2) shows a mode near 500Hz. We set a target bandwidth of 150 Hz since actuator-saturation limitations make control implementations impractical for bandwidths beyond that. As discussed in section 1 and 3.1, we imposed robustness to modeling uncertainties as an objective. Also, consideration for noise requires high priority for control design since signals in small scale can be easily buried in noise. Thus noise attenuation decides the resolution. To attenuate high frequency noise, we impose an objective of having small noise effecting frequency and having a second order roll-off rate for closed loop transfer function of the device. The objectives and limitations on the control design are better explained in terms of the schematic shown in Figure 3(a).

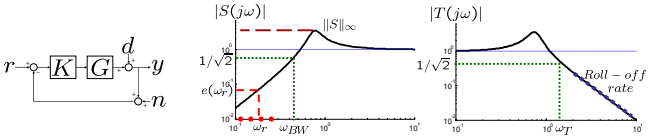

(a) (b)

Fig. 3. (a)Servo feedback configuration. (b)Objectives of feedback control. The objectives of the control design is to achieve high tracking bandwidth (by designing for large ω_{BW}), high precision (by achieving smaller error $e(\omega_r)$ at reference frequencies ω_r and attenuating the noise through high roll-off rate and small roll off frequency ω_T) and robustness (by achieving $\|S\|_\infty$ close to 1).

The error is given by $e = r - x = Sr - Sd + Tn$, where the sensitivity function S is defined by $S = 1/(1 + GK)$ and the complementary sensitivity function T is defined by $T = 1 - S$. The closed-loop tracking bandwidth is defined as the frequency at which $|S(j\omega)|$ crosses -3 dB. Since S is the transfer function from r to e for feedback control, the bandwidth can be used as a measure of tracking capability where error remains relatively smaller than reference signal(Skogestad and Postlethwaite (2005)). $\|S\|_\infty$ is employed as a measure of the robustness to modeling uncertainties and is used for comparing robustness of various design schemes. The objectives on the control design are summarized in Figure 3(b).

3.3 Limitations

These objectives have to be achieved under some practical and fundamental limitations. For instance, practically the sampling period can never be faster than the time required by DSP to calculate steps in control logic. Thus both high frequency sampling and high order control logic can not be achieved simultaneously. According to the discrete time control theory, more than 30 times of frequency range of interest is required for sampling frequency for discrete control (Franklin et al. (2005)). Also, signal generated by controller can not be larger than the saturation limits of the hardware (−10 to 10V). Besides the above practical limitations, the simultaneous achievement of objectives becomes difficult due to algebraic limitations on the control design. The fundamental algebraic limitations for feedback design arise as follows. The limitation $S + T = 1$ prevents error $e = r - x = Sr - Sd + Tn$ from becoming small in all frequencies since S and T can not be made small simultaneously. This motivates search for control designs that achieve a tradeoff between the bandwidth and resolution requirements. Besides, for open loop systems with phase margin less than 90 deg which include most practical systems, the bandwidth ω_{BW} cannot be larger than ω_T as shown in Figure 3(b) (Skogestad and Postlethwaite (2005)). This blocks the feedback control to achieve noise attenuation over target reference frequency range. Another limitation which imposes a trade-off between the bandwidth, the resolution and the robustness requirements can be explained in terms of the Bode integral law (Freudenberg and Looze (1985)). While designing the feedback controller, the performance object of high bandwidth with a small tracking error, and the robustness condition cannot be satisfied simultaneously. Since T needs a sufficiently fast roll off rate at high frequencies for noise attenuation, the open loop transfer function $K(s)G(s)$ has greater than or equal to relative degree of order 2, the Bode integral law for a stable system, $\int_0^\infty \log|S(j\omega)|d\omega = 0$ needs to be satisfied. Moreover, the equation (1) reveals a real non-minimum phase zero and a stricter condition is imposed by another law $\int_0^\infty \log|S(j\omega)|\, W(z,\omega)d\omega = 0$ where $W(z,\omega) = \frac{2z}{z^2+\omega^2}$ for real positive pole z.
This Bode law (for the given system) displays a *finite waterbed effect* where it can be shown that the area of $\log|S(j\omega)|$ over a *finite* frequency region can be bounded from below. Thus the simultaneous requirements of low $|S(j\omega)|$ over a large frequency for a high tracking bandwidth, high order roll off rates of T at high frequencies for high resolution and small peaks of $S(j\omega)$ for robustness to modeling uncertainties compete against each other under this limitation. For instance small $|S(j\omega)|$ over a specified bandwidth might not leave out enough frequency range to zero out the area in the 'finite water bed effect' even with $S(j\omega)$ at the allowed peak value for the remaining frequencies.

4. CONTROL DESIGN

In this section, we first show the results obtained from designs typically used in AFM industry and then compare them with the results obtained from the proposed design. The design presented wraps around the existing controller to make the resulting system more robust to modeling uncertainties and have higher bandwidth. This restriction in design is motivated by the practical limitation where the commercial controllers are sometimes hardwired to deliver certain performance goals (such as tracking ramps).

4.1 PII control design

Proportional-integral (PI) and proportional-integral-integral (PII) controllers are the most common type controllers currently used in commercial scanning-probe microscope. Their popularity stems from the fact that they are simple to implement, and easy for people with no control background to develop a feel for tuning. Furthermore, their design philosophy is independent of the plant model and in that sense they are simple. Moreover, PII controllers track ramp signals, which can partially represent raster scan, with zero steady-state error. The PII controller has the structure $K_{PII} = k_p + \frac{k_i}{s} + \frac{k_{ii}}{s^2}$.

This non model based controller design requires an exhaustive search over the space of controller parameters to meet bandwidth and robustness requirement. In this paper, k_p was chosen as 0 to get the roll off of 40 dB/dec in high frequency noise attenuation and the design of parameters k_i and k_{ii} was done exhaustively by finding the bandwidths and $\|S\|_\infty$ by simulating a fine grid of points (100 points per each parameter) that represented all possible stabilizing PII controllers. The results are shown in Figure 4. Selection of parameters outside the colored region renders the resulting closed-loop systems unstable.

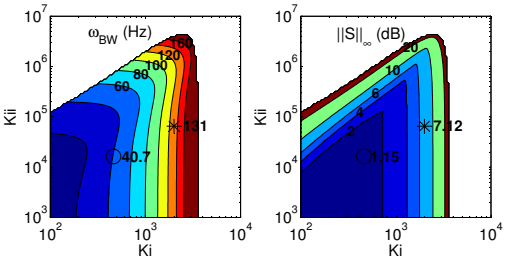

Fig. 4. Simulation results of Design of Parameter for bandwidth and $\|S\|_\infty$: Robust PII control (o) has bandwidth of 40.7 Hz, and $\|S\|_\infty$ of 1.15dB. Aggressive PII control (*) has bandwidth of 131 Hz and $\|S\|_\infty$ of 7.12dB.

As seen in Figure 4, ω_{BW} and $\|S\|_\infty$ requirements conflict with each other i.e. good performance and robustness cannot be achieved simultaneously. This corresponds the Bode integral law described in section 3. To compare the performance and robustness, 2 PII controllers are chosen - Robust controller $K_{rPII} = \frac{462.33}{s} + \frac{16287}{s^2}$ (o in Figure 4) which is conservative in stability robustness but the bandwidth is limited and not appropriate the high speed scanning and Aggressive controller $K_{aPII} = \frac{2\times10^3}{s} + \frac{6.5\times10^4}{s^2}$ (* in Figure 4) which has 3 times higher bandwidth but has low robustness.

4.2 Two degree of freedom controller

To achieve the high bandwidth robust positioning, a two degree of freedom (2DOF) controller is designed based on existing PII controllers typically employed in nanopositioners.

While conventional feedback control is designed on the difference between reference input and measured output i.e. $u = K(r - y)$, the 2DOF control acts on the reference input and the measured output signal separately i.e. $u = K_1 r + K_2 y$ (see Figure 5). We employ a 2DOF model matching design which has the goal to make the transfer function of the closed loop device match a pre-specified target transfer function T_{ref} (Hoyle et al. (1991); Limbeer et al. (1993)).

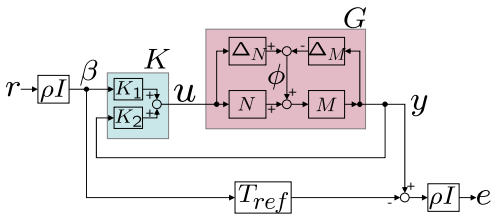

Fig. 5. Two degree of freedom control configuration.

The design process needs plant shaping first and robustification and model matching was done on this shaped plant. The procedure is analogous to the Glover-McFarlane 2 step design (plant shaping and robustfication in Glover and McFarlane (1989)) but utilizing the additional freedom acquired from using two separate control laws, model matching is integrated in robustifcation process. Glover-MacFarlane loop shaping achieves robustness of system to modeling uncertainties without compromising the performance and model matching achieves an increase in the bandwidth through feedforward and feedback control.

Step 1) **Plant shaping:** A shaping transfer function W_s was designed based on conventional one degree of freedom framework. This shape function will supply the basic structure of controller such as relative order or roll-off rate and performance of closed loop system. Though the performance of closed loop transfer function is determined in this step for Glover-McFarlane procedure, transfer function from r to y will be reshaped through model matching in step 2. However, the other transfer functions such as d to y or n to y remain unaffected by the model matching. In the design presented in this paper, W_s is set equal to PII controllers chosen in section 3 so that the shaped plant has the transfer function of $G_s = W_s G_{xx}$. This choice is to retain the closed-loop property of tracking ramp signals without steady-state error.

Step 2) **Two degree of freedom control design:** A controller $K = [K_1\ K_2]$ is obtained simultaneously by posing and solving an appropriate $\mathcal{H}_\infty$ optimal control problem. K_1 and K_2 are designed so that the closed loop system from shaped plant in step 1 has good robustness and so that the transfer function from r to y has similar response with the given reference transfer function. The shaped plant is given as $G_s = M^{-1}N$ through coprime factorization. In this setting, the control design aims at robustness to modeling uncertainty by ensuring the stability of all plants in the set

$$\{G_p | G_p = (M - \Delta_M)^{-1}(N + \Delta_N), \|[\Delta_M\ \Delta_N]\|_\infty \le \frac{1}{\gamma}\} \qquad (2)$$

where γ specifies a bound on the uncertainty.

The desired closed-loop transfer function T_{ref} is selected by the designer to satisfy the response characteristics. The parameter ρ determines the emphasis between model matching and robustification in optimization. (if ρ is 0 then problem becomes the Glover-McFarlane design problem). The optimization problem is to find the stabilizing

controller $K = [K_1\ K_2]$ for the shaped plant G_s which minimizes the $\mathcal{H}_\infty$ norm of the transfer function between $[r\ \phi]^T$ and $[u\ y\ e]^T$. The corresponding system is given by

$$\begin{bmatrix} u \\ y \\ e \end{bmatrix} = \left[\begin{array}{cc|c} \rho K_1 S & & K_2 S M^{-1} \\ \rho G_s K_1 S & & S M^{-1} \\ \hline \rho^2(G_s K_1 S - M_0) & & \rho S M^{-1} \end{array}\right] \begin{bmatrix} r \\ \phi \end{bmatrix} \quad (3)$$

where $S = (1 - G_s K_2)^{-1}$.

The generalized plant P is given by

$$\begin{bmatrix} u \\ y \\ e \\ \hline \beta \\ y \end{bmatrix} = \left[\begin{array}{cc|c} 0 & 0 & I \\ 0 & M^{-1} & G_s \\ -\rho^2 T_{ref} & \rho M^{-1} & \rho G_s \\ \hline \rho I & 0 & 0 \\ 0 & M^{-1} & G_s \end{array}\right] \begin{bmatrix} r \\ \phi \\ u \end{bmatrix} \quad (4)$$

and used in $\mathcal{H}_\infty$ synthesis to find the controller $[K_1\ K_2]$.

However, the additional step is required to improve the tracking performance. As a final refinement for tracking problem, K_1 need to be scaled so that closed-loop transfer function matches the reference transfer function at steady state problem. Scale W_0 is defined as $W_0 = S(s)[G_s(s)K_2(s)]^{-1}T_{ref}\big|_{s=0}$ and the resulting controller becomes $K = [K_1 W_0 \quad K_2]$

4.3 Robustification and model matching of aggressive PII controller

The design process was applied to G_{xx} with W_s as K_{aPII} in section 3, ρ as 5, T_{ref} as $\frac{1}{0.00035s+1}$. The two degree of freedom controller was obtained as

$$\begin{aligned} K_{2DOF} &= KW_s = [K_{TD1}\ K_{TD2}] \\ K_{TD1} &= \frac{8.146 \times 10^{10}(s+32.51)(s+32.5)}{s^2(s+5.914\times10^6)(s+2857)(s+961.8)} \\ &\times \frac{(s^2+1788s+9.264\times10^5)(s^2+236.5s+9.937\times10^6)}{(s+32.5)(s^2+154.6s+9.925\times10^6)} \\ &\times \frac{(s^2+708.3s+1.168\times10^7)(s^2+3338s+2.469\times10^7)}{(s^2+375.4s+1.454\times10^7)(s^2+9967s+6.354\times10^7)} \quad (5) \\ K_{TD2} &= \frac{-4.062\times10^{10}(s+749.8)(s+32.5)}{s^2(s+5.914\times10^6)(s+961.8)} \\ &\times \frac{(s+31.62)(s^2+259.9s+1.017\times10^7)}{(s+32.5)(s^2+154.6s+9.925\times10^6)} \\ &\times \frac{(s^2+863.4s+1.063\times10^7)(s^2+3119s+2.363\times10^7)}{(s^2+375.4s+1.454\times10^7)(s^2+9967s+6.354\times10^7)} \end{aligned}$$

For 2DOF case, the transfer functions from r to y and from n to y are different which is a great advantage of 2DOF controller thus it is needed to distinguish them. In the remainder of the paper, T denotes the transfer function from n to y, $S = 1 - T$, T_{ry} denotes the transfer function from r to y and S_{re} denotes the transfer function from r to e, i.e. $S = \frac{1}{1-GK_2}$, $T = \frac{GK_2}{1-GK_2}$, $S_{re} = S(1 - GK_1 - GK_2)$, $T_{ry} = SGK_1$, thus $y = T_{ry}r + Tn + Sd$, $e = S_{re}r - Tn - Sd$.

Figure 6(a) compares the sensitivity function $S(s)$ and the complementary sensitivity function $T(s)$ of feedback control and 2DOF control. $S(s)$ in 2DOF design represents the robustness of closed loop system thus the graph shows the improvement in robustness($\|S\|_\infty$ =2.27(feedback) 1.32(2DOF)). $T(s)$ in 2DOF represents the influence of the noise thus it reveals the 2DOF attenuates more noise.

Figure 6(b-upper) compares the transfer function from reference to error i.e. $S(s)$ of feedback controller and S_{er} of

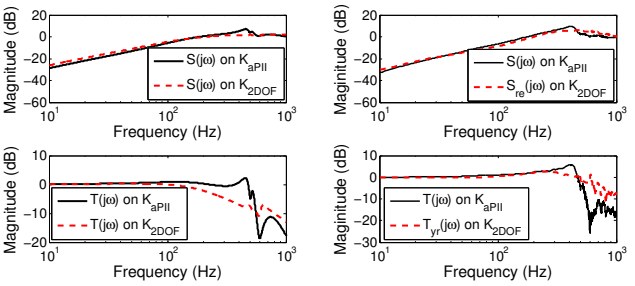

(a) (b)

Fig. 6. (a)Bode plot of $S(s)$ and $T(s)$: 2DOF control has better robustness(upper) and better noise attenuation(bottom). (b)Experimentally calculated bode plot of $S(s)$ and $S_{er}(s)$, $T(s)$ and $T_{yr}(s)$: 2DOF and agressive PII control show similar bandwidth(upper).

2DOF control. $S_{er}(s)$ in 2DOF design represents the tracking performance (ω_{BW}=141Hz(feedback) 161Hz(2DOF)). Figure 6(b-lower) also compares the transfer function from reference to output i.e. $T(s)$ of feedback controller and $T_{yr}(s)$ of 2DOF control.

4.4 Robustification and model matching of robust PII controller

The same design process was applied to G_{xx} with W_s as K_{rPII} in section 3. ρ as 5 and T_{ref} as $\frac{1}{0.0003s+1}$. Similar to (5), a 2DOF controller (12th order law for K_{TD1} and 11th order law for K_{TD2}) was obtained. In this case, $S(s)$ in 2DOF design shows almost similar robustness (Figure 7(a) $\|S\|_\infty$ =1.14(feedback) 1.12(2DOF)) and also noise attenuation in 2DOF design is almost same with feedback design case because the feedback system is already robust thus 2DOF design did not make much improvement in robustness and noise attenuation.

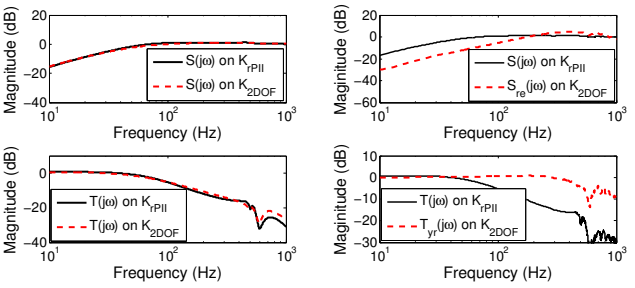

(a) (b)

Fig. 7. (a)Bode plot of $S(s)$ and $T(s)$: 2DOF and robust PII control have similar robustness(upper) and noise attenuation(bottom). (b)Experimentally calculated bode plot of $S(s)$ and $S_{er}(s)$, $T(s)$ and $T_{yr}(s)$: 2DOF control has higher bandwidth(upper).

However, $S_{er}(s)$ in 2DOF design shows the improvement in tracking performance.(Figure 7(b) ω_{BW}=40Hz(feedback) 128Hz(2DOF)).

5. ANALYSIS AND DISCUSSION

The 2DOF design is not bound by some fundamental limitations that constrain the feedback-only designs. For instance, in feedback-only design the tracking bandwidth

ω_{BW} can never be made larger than the roll off frequency ω_T which determines how much noise is fed back and hence the resolution. This gives a strict trade-off between the resolution and the bandwidth. However, the results in section 4 shows that in 2DOF design, ω_{BW} of the closed loop device can be made larger than ω_T. 2DOF control based on robust PII controller has ω_{BW} of 128Hz and ω_T of 80Hz while original robust PII controller has the bandwidth of 40Hz and the noise bandwidth of 81Hz. (The 2DOF control based on aggressive PII controller case, ω_T is still smaller than ω_{BW} but this comes from the target bandwidth for the design.)

The 2DOF design has greater freedom than feedback-only design with respect to Bode integral laws, hence obtains better tracking bandwidth. Figure 8(a) shows the bode diagram for $K_{2DOF}(s) = [K_{TD1}(s)\ K_{TD2}(s)]$ in 2DOF control based on aggressive PII controller. Note that, in low frequencies, the control law is essentially feedback-only since K_{TD1} and K_{TD2} have almost same magnitude and are 180 degree out of phase, i.e. $K_{TD1} \approx -K_{TD2}$, and therefore $u \approx K_{TD1}(r - y)$. The 2DOF nature of the control becomes active at high frequencies ($>$ 130 Hz) where the feedforward part is more dominant. The analytical prediction of this separation is being currently pursued. This separation is more dominant in 2DOF control based on robust PII controller (Figure 8(b)).

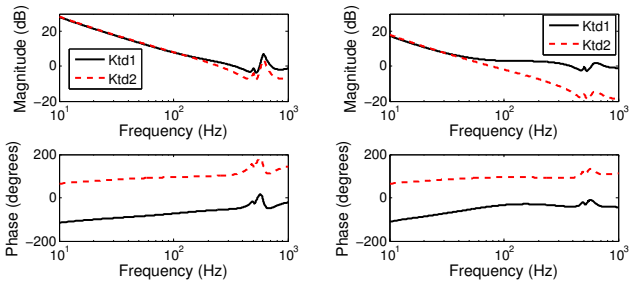

Fig. 8. Bode plot $K_{2DOF}(s) = [K_{TD1}(s)\ K_{TD2}(s)]$: 2DOF control nature becomes active at high freqeuncy (a)2DOF controller based on aggressive PII controller (b)2DOF controller based on robust PII controller

6. CONCLUSION

This paper describes a new procedure for a systematic control design and analysis of nano-positioners. In nano-positioners, along with high bandwidth and high resolution, robustness assumes great significance. A robust linear controller is needed to tackle the nonlinearities associated with piezoactuation and the changing flexure dynamics without having to design specific nonlinear controllers. The design goals of robustness, bandwidth and resolution can be quantified in a straightforward manner in the framework of modern robust control. Two degree of freedom control design is employed to improve the bandwidth of controllers and robustness simultaneously while maintaining the resolution requirements. Two degree of freedom control design developed by Limbeer et al. (1993) includes the robustfication and the model matching in the $\mathcal{H}_\infty$ optimization. These design methodologies are experimentally demonstrated on a nano-positioner. The analytic and experimental sensitivity and complementary sensitivity functions along with tracking results demonstrate the merits of the design. The 2DOF design is shown to achieve performance characteristics that were impossible by feedback-only designs.

REFERENCES

B. Bhushan. *Handbook of Micro/Nano Tribology*. CRC Press, 2nd edition, 1999.

D. Croft, G. Shedd, and S. Devasia. Creep, Hysteresis and Vibration compensation for Piezoactuators: Atomic Force Microscopy Application. In *Proceedings of the American Control Conference*, pages 2123–2128, June 2000.

A. Daniele, M. V. Salapaka, S. Salapaka, and M. Dahleh. Piezoelectric scanners for atomic force microscopes: design of lateral sensors, identification and control. In *Proceedings of the American Control Conference*, pages 253–257, June 1999.

H.L. Fillmore, I. Chasiotis, S.W. Cho, and G.T. Gillies. Atomic force microscopy observations of tumour cell invadopodia: novel cellular nanomorphologies on collagen substrates. *Nanotechnology*, 14:73–76, 2003.

G.F. Franklin, J.D. Powell, and M. Workman. *Digital Control of Dynamic Systems*. Pearson Education, 3rd edition, 2005.

J. S. Freudenberg and D. P. Looze. Right half-plane poles and zeros and design tradeoffs in feedback systems. *IEEE Transactions on Automatic Control*, 30(6):555–565, 1985.

K. Glover and D. McFarlane. Robust stabilization of normalized coprime factor plant descriptions with $\mathcal{H}_\infty$-bounded uncertainty. *IEEE Transactions on Automatic Control*, 34(8):821–830, August 1989.

D.J. Hoyle, R.A Hyde, and D.J.N. Limbeer. An $\mathcal{H}_\infty$ approach to two degree of freedom design. In *Proceedings of the IEEE Conference on Dicision and Control*, pages 1581–1585, December 1991.

K. Leang and S. Devasia. Hysteresis, creep and vibration compensation for piezoactuators: feedback and feedforward control. In *Proceedings of 2nd IFAC Conference on Mechatronic Systems*, pages 283–289, 2002.

D.J.N. Limbeer, E.M. Kasenally, and Perkins J.D. On the desing of robust two degree of freedom controllers. *Automatica*, 29(1):157–168, 1993.

S. Salapaka, A. Sebastian, J. P. Cleveland, and M. V. Salapaka. High bandwidth nano-positioner: A robust control approach. *Review of Scientific Instruments*, 73 (9):3232–3241, 2002.

G. Schitter, P. Menold, H. F. Knapp, F. Allgower, and A. Stemmer. High performance feedback for fast scanning atomic force microscopes. *Review of Scientific Instruments*, 72(8):3320–3327, August 2001.

G. Schitter, F. Allgower, and A. Stemmer. A new control strategy for high speed atomic force microscopy. *Nanotechnology*, 15(1):108–114, 2004.

A. Sebastian and S. Salapaka. Design methodologies for robust nano-positioning. *IEEE Transactions on Control Systems Technology*, 13(6):868–876, 2005.

S. Skogestad and I. Postlethwaite. *Multivariable Feedback Control, Analysis and Design*. John Wiley and Sons, 2nd edition, 2005.

Wu Y. and Q. Zou. Iterative control approach to compensate for both the hysteresis and the dynamics effects of piezo actuators. *IEEE Transaction on Control Systems Technology*, 15(5):936–944, September 2007.